Catalysis Today 166 (2011) 39–46

Contents lists available at ScienceDirect

Catalysis Today

journal homepage: www.elsevier.com/locate/cattod

3D net-linked mesoporous silica monolith: New environmental adsorbent and catalyst

Yu Zhou[a], Fang Na Gu[a,b], Ling Gao[a], Jia Yuan Yang[a], Wei Gang Lin[a], Jing Yang[a], Ying Wang[b], Jian Hua Zhu[a,*]

[a] Key Laboratory of Mesoscopic Chemistry of MOE, College of Chemistry & Chemical Engineering, Nanjing University, Nanjing 210093, China
[b] Ecomaterials and Renewable Energy Research Center (ERERC), Nanjing University, Nanjing 210093, China

ARTICLE INFO

Article history:
Available online 5 July 2010

Keywords:
SBA-15 mesoporous silica
Morphology
Selectivity adsorption
Catalytic degradation
Tobacco specific nitrosamines
Environment protection

ABSTRACT

This paper reported the synthesis, characterization, adsorption and catalysis of new morphology-assisted functional SBA-15, the 3D net-linked mesoporous silica monolith, and its actual function in selective reducing tobacco specific nitrosamines (TSNA) level of smoke, in order to explore the new route elevating the efficiency of environment adsorbents/catalysts through their morphology controlling. It is feasible to control the hydrolization and condensation of silica source in synthesis, and then piloting the formation and the secondary arrangement of primary particles, finally forming the monolith with 3D net-linked morphology. The resulting sample not only had the shape of monolith, but also possessed a considerable mechanical intensity hence it could be directly sieved for use without molding. With the assistant of net-linked morphology, this monolith sample could intercept the particles with μm sizes in tobacco smoke, and selectively capture the TSNA adhered on the particle, providing new functional material for environment protection. Through dry-impregnation it is also successful to modify the monolith with zirconia guest without damage of 3D net-linked morphology, dramatically increasing the activity of the composite in the instantaneous adsorption of volatile nitrosamine such as *N*-nitrosopyrrolidine (NPYR) and the temperature programmed surface reaction (TPSR) of *N*′-nitrosonornicotine (NNN), offering a powerful environmental catalyst to degrade carcinogenic pollutants.

1. Introduction

Design and synthesis of new materials are crucial for catalysis and adsorption, especially for environmental adsorption and catalysis because of their strict requirements. Unlike traditional industrial adsorption, environmental adsorption faces complex system in which trace amount of target such as carcinogenic pollutants is wrapped within numerous other components with large volumes, and one typical example is to eliminate the carcinogens in environment tobacco smoke (ETS). The relation between smoking and health hazard has been well established, but it is hard to control the pollution caused by smoking. Apart from anti-smoking campaigns, a lot of effort has been devoted to trap the pollutants in ETS. Tobacco smoke consists of more than 5000 kinds of compounds, among them nitrosamines, volatile nitrosamines and tobacco specific nitrosamines (TSNA) characterized with functional group of N–NO, are carcinogenic to cause serious health risk even in trace amounts [1,2]. TSNA are the most abundant carcinogens identified in tobacco and tobacco smoke, including *N*′-nitrosonornicotine (NNN), 4-methylnitrosarnino-1-3-pyridyl -1-butanone (NNK), *N*′-nitrosoanatabine (NAT), and *N*′-nitrosoanabasine (NAB), and they are likely to play an important role as causative agents in cancer of the esophagus, pancreas, and oral cavity associated with smoking. Nonetheless, it is unfathomable to trap TSNA in smoke by microporous materials such as zeolites and mesoporous silica [3,4], though these materials could adsorb and degrade TSNA in laboratorial experiments [5,6]. The inferior performance may result from 2 reasons: one is the complex composition of tobacco smoke that easily contaminates the active sites of adsorbent, and another is that most TSNA species exist in the particular phase of smoke, and the size of these particles achieve μm grade [7], exceeding the pore diameters of zeolites and mesoporous materials. In contrary, cellulose acetate in the filter of cigarette was able to reduce the TSNA level of smoke through physically intercepting the particles [8], but it could not selectively trap TSNA. Activated carbon, especially the microporous activated carbon made from coconut, could also reduce the TSNA level of smoke through trapping the particles in smoke, of course, it also lacked the selectivity to trap TSNA [3]. Recently, we reported the first morphology-assisted functional material, the calcosilicate CAS-1 with fiber-like morphology, to trap the particles in smoke and more important [3], CAS-1 seemed to show the selectivity toward TSNA

* Corresponding author. Tel.: +86 25 83595848; fax: +86 25 83317761.
E-mail address: jhzhu@netra.nju.edu.cn (J.H. Zhu).

0920-5861/$ – see front matter © 2010 Elsevier B.V. All rights reserved.
doi:10.1016/j.cattod.2010.04.052

in adsorption although there was no deep investigation on this phenomenon.

Selective adsorption is essential for catalytic reaction in complicated conditions such as environmental catalysis. By now, great efforts had been made to create active sites on mesoporous silica materials to improve their adsorption and catalytic performances [9–11]. However, few are focused on the study how to create and tune the selectivity of mesoporous silica materials by their morphology controlling at micro-scale and macro-scale levels. CAS-1 had the interlaced fiber-like morphology [12], different from traditional zeolites with powder-like morphology. Besides, CAS-1 had two-dimensional eight-ring channel system [13], plus two cations (Ca^{2+} and K^{+}) in its structure, which might have contribution on the adsorption toward TSNA so the reason to cause the TSNA selectivity became unclear. To deeply explore the influence of morphology on the selective adsorption of mesoporous silica, it is necessary to obtain the samples with same chemical composition and porous structure but different morphology. Fortunately, we successfully prepared a kind of SBA-15 with monolithic shape in macroscopic view, 3D net linked micromorphology at micrometer level and ordered mesoporous channel of 9 nm [14], and it also displayed superior performance in eliminating tar and nitrosamines in smoke. Since this material owns almost the same textural properties as SBA-15, and its surface modification is facile, it is chosen to further study the influence of morphology on environmental adsorption and catalysis. Moreover, we want to find the mechanism why the special morphology enables the functional material to realize the selective trapping TSNA in smoke, through which we hope to get clue for developing new material with high efficiency to protect environment.

In present work, we continue the synthetic route reported previously [14] to prepare the SBA-15 mesoporous silica with different morphology, and examine their adsorption and catalytic properties in laboratorial tests. Two nitrosamines, *N*-nitrosopyrrolidine (NPYR) and *N*′-nitrosonornicotine (NNN), the former is a typical volatile nitrosamine and the latter is one kind of TSNA, are chosen to be the probe in instantaneous adsorption or liquid adsorption along with the temperature programmed surface reaction (TPSR) or in situ FTIR measurements. Moreover, these mesoporous materials will be directly put into the filter of cigarette to trap the particles and TSNA in smoke, in order to assess their actual function in environmental adsorption and to examine the contribution of morphology controlling on the selectivity in adsorption. To elevate the performance of mesoporous silica, we would try to modify the material with metal oxide guest through a special impregnation method because we need to preserve the special morphology of the host, and zirconia is selected as the modifier based on its success in modifying zeolites [15]. The resulting composite is also tested in the gaseous adsorption, liquid adsorption and TPSR test of nitrosamines, in order to assess its actual function in eliminating the carcinogenic pollutants.

2. Experimental

2.1. Materials

NPYR, NNN, NNK, NAB and NAT were purchased from Sigma, and their structures were shown in Fig. S1. The purity of N_2 and H_2 carrier gases was 99.99%, and all other agents used here were of AR grade. The Virginia type cigarette was purchased from market.

Mesoporous silica SBA-15 was synthesized according to literature [16]. Typically, 3.0 g of P123 block copolymer was dissolved in the aqueous solution containing 22.5 g of water and 90 g of HCl (2 M), and then 6.38 g of tetraethyl orthosilicate (TEOS) was added with vigorous stirring at 313 K. After being stirred at 313 K for 24 h, the gel solution was transferred into a Teflon bottle and heated at 373 K for 24 h without stirring. The solid product was recovered by filtering, washed with deionized water, air-dried and finally calcined at 773 K for 5 h. The 3D net-linked mesoporous silica, SM sample, was synthesized similarly, with a slow stirring rate and tetramethyl orthosilicate (TMOS) instead of TEOS, as previous described [14]. SM-P sample was prepared by pressing the calcined SM sample with the pressure of 2 MPa. To prepare the sample 5% ZrO_2/SM through dry-impregnation process, the calculated amount of zirconium nitrate ($Zr(NO_3)_4{\cdot}9H_2O$) was dissolved in 10 mL deionized water, and then uniformly dipped on 1 g synthesized SM sample. The obtained solid was air-dried and then calcined at 773 K in air flow for 5 h.

2.2. Measurements

X-ray diffraction (XRD) patterns were recorded on an ARL XTRA diffractometer in the 2θ range of 0.6–5°. Scanning electron microscopy (SEM) images of sample were obtained with HITACHI S4800 microscopes. The sample disc was coated with Au film prior to imaging to improve the conductivity. The BET specific surface area was calculated using adsorption data acquired at a relative pressure (P/P^0) range of 0.05–0.22 and the total pore volume was determined from the amount adsorbed at a relative pressure of about 0.99. The micropore area, S_{mic}, and micropore volume, V_{mic}, were calculated by the *t*-plot method, according to the statistical film thickness (t) in the range of 0.35–0.50 nm. The pore size distribution (PSD) curves were calculated from the analysis of the adsorption branch of the isotherm using the Barrett–Joyner–Halenda (BJH) algorithm.

In situ FTIR investigation was performed in a purpose-built IR cell with CaF_2 windows, and a Bruker 22 FTIR spectrometer with a resolution of 2 cm^{-1} was used. The sample with an area density of 10 mg cm^{-2} was slowly heated to 423 K in N_2 flow. After the temperature was stable, a background spectrum was collected. Subsequently, 30 μL NNN solutions (5 mg mL^{-1}) were injected into the IR cell and then IR spectra were collected after 15 min.

Instantaneous adsorption of NPYR in gaseous phase was performed in a fixed-bed micro-reactor filled with 5 mg samples (20–40 meshes), and the sample was directly heated to 453 K without activation in the flow of H_2 with a rate of 20 mL min^{-1}. Nitrosamine solution was pulse injected with 2 μL each time, and the gaseous effluent was analyzed by a gas chromatograph [14]. Liquid adsorption of NNN was completed at 277 K, and 20 mg sample particles in 20–40 meshes contacted with 1.1 mL dichloromethane solution of NNN for 24 h. The residual nitrosamines in solution were detected by spectrophotometer [17]. Temperature program surface reaction (TPSR) was performed in the manner reported previously [18]. Twenty mg samples (20–40 mesh) were activated in N_2 flow at 773 K for 2 h and then cooled to 313 K, followed by the injection of 100 μL solution of NPYR (55 μmol). After the sample was purged on N_2 flow for 0.2 h, it was heated to 773 K at a rate of 8 K min^{-1} while the gaseous cracking products were detected every 20 K by spectrometric method [17].

To evaluate the function of sample in reducing TSNA level of smoke, the sample with calculated amount (20–40 meshes) was added into the filter of cigarette to replace part of cellulose matrix with a same volume [3]. The 20–40 mesh particles of SM and 5% ZrO_2/SM were obtained by directly sieving the calcined sample, for other materials they were firstly pressed under 2 MPa then divided and sieved. Twenty cigarettes were conditioned at 295 K and 60% relative humidity for 48 h and then smoked using a Borgwaldt smoking machine RM20/CS under the standard ISO machine-smoking regime (35 cm^3 puff, 2 s duration every 60 s [19]). Each Cambridge filter pad with trapped smoke particulate was extracted by 50 mL ammonium acetate solution in ultrasonic for 30 min, further purified using the GX-274 ASPEC autosolid-phase

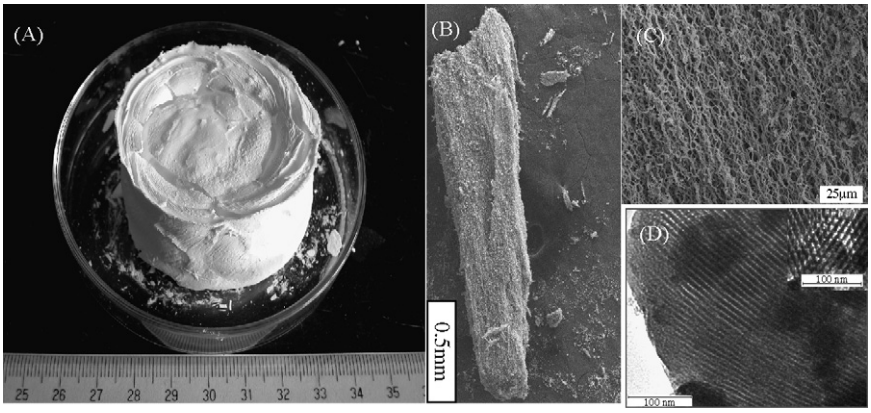

Fig. 1. The optical (A), SEM (B and C) and TEM (D) images of calcined SM sample.

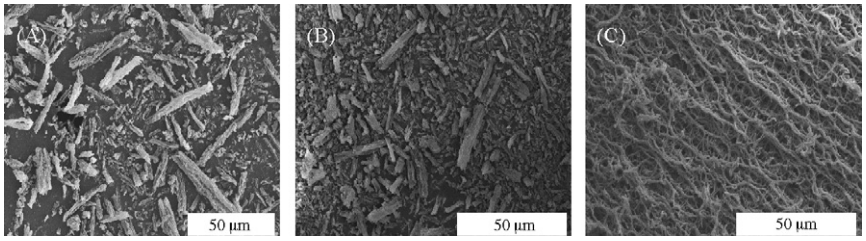

Fig. 2. SEM images of (A) SBA-15, (B) SM-P and (C) 5% ZrO_2/SM samples.

extraction machine and finally analyzed by Agilent 1200 LC system and 6410 Triple Quad LC–MS/MS [3].

3. Results

3.1. Structure characterization

Fig. 1 demonstrates the macroscopic and microscopic morphology of SM sample. Different from SBA-15 mesoporous silica with powder-like macroscopic shape [16], SM sample is large monolith with a diameter of about 40 mm and a height of 30 mm. This macroscopic difference is induced from the different micromorphology of two samples. SBA-15 was wheat-like with the length several micrometers to tens of micrometers (Fig. 2A and Fig. S2A). SM sample owned the same primary rod-like particles as SBA-15 (Fig. S2B), but these rods run parallel to the long axis end to end, forming fiber-like secondary microphology, as shown in Fig. 1C; The magnified SEM image was also illustrated in Fig. S2B. Then, different from SBA-15 fibers reported previous [20,21], these secondary fiber-like particles of SM sample were parallel-aligned and cross-linked with each other to form three-dimensional netlike aggregations, yielding monolithic macromorphology (Fig. 1). Detailedly, the main difference of SM and SBA-15 in microscopic view was the senior configuration of primary particles. Both samples contained the secondary rope structure formed by coupling of the primary rods from one end to the other [20]. The ropes of SBA-15 run parallel and closely arranged to form bundles, the regular two-dimensional aggregations [22,23], with various length of tens of micrometers; while the ropes of SM were uniformly dispersed and cross-linked to form net-like framework in three dimensions throughout the whole sample. It is the ordered conformation extending to a long range (centimeter) in three dimensions that yielded the special monolithic shape of SM sample. Moreover, this regulation from microscopic to macroscopic level not only provided the net-linked configuration in whole product, but also strengthened the toughness of sample. The sample of SM could keep its monolithic shape under the force of 2.5 N cm^{-2}, and broke to several blocks in higher pressure. The material was partly pulverized around the pressure of 10 N cm^{-2}, and finally, the 3D net linked framework became ruined at the pressure of 2 MPa, giving the sample of SM-P. As the SEM image revealed (Fig. 2B), the resulting sample SM-P lost the net framework but kept the primary particles. Through the careful dry impregnation, it was possible to adjust the surface states of SM without damage of its special structure. For instance, zirconia could be uniformly dispersed on the surface of SM while the morphology was conserved. 5% ZrO_2/SM was still block to own the 3D net-linked framework, as demonstrated by SEM measurement (Fig. 2C).

Fig. 3 displays the low-angle X-ray diffraction patterns of SBA-15, SM, SM-P and 5% ZrO_2/SM samples. Although monolithic SM owned 3D net-linked framework, it still had the same low-angle XRD pattern as SBA-15. The XRD patterns consisted of

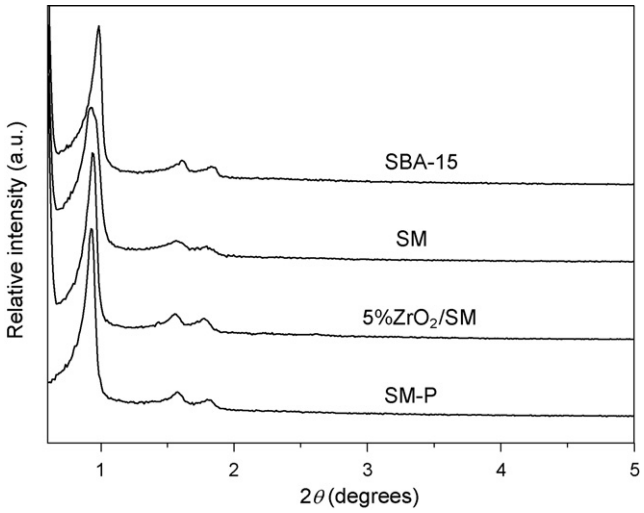

Fig. 3. Low angle XRD patterns of mesoporous silica SBA-15.

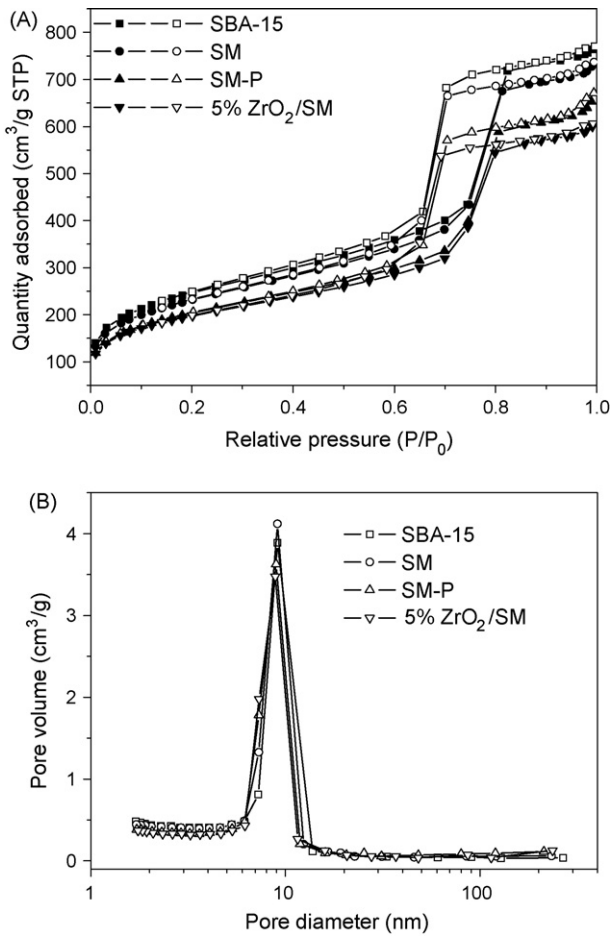

Fig. 4. (A) N_2 sorption isotherms and (B) pore size distribution of mesoporous silica samples.

one high-intensity reflection and two higher-angle ones indexed as (100), (110) and (200), respectively, and the values of $d(100):d(110):d(200)$ are $1:\sqrt{3}:2$, indicating a well-ordered mesostructure of 2D hexagonal symmetry (*p6mm*) [16] that was further conformed by TEM image (Fig. 1D). Post treatment of SM with high pressure or dry-impregnation did not change the symmetry, both SM-P and 5% ZrO_2/SM samples kept the parent symmetry (Fig. 3).

Fig. 4 illustrates the nitrogen sorption results of SBA-15, SM, SM-P and 5% ZrO_2/SM samples, and Table 1 lists their textual properties. All N_2 adsorption–desorption isotherms were type IV with a well-resolved type-H1 hysteresis loop characteristic of typical (1D) cylindrical channel mesoporous materials [24]. Also, they all yielded a narrow pore-size distribution with a mean value of around 9.0 nm from the adsorption progress, mirroring the almost same textual structure of SM to SBA-15. After SM was pressed in 2 MPa, its surface area and pore volume decreased, due to the collapses of some channels under high pressure, but the most probable pore size unchanged. Zirconia modification also made the surface area and total pore volume of SM sample declined, because of the existence of guest modifier within channels, similar to that observed in CuO modified SBA-15 [6].

As mentioned above, the only difference between SBA-15 and SM samples was the secondary micromorphology since two samples possessed the similar textural properties such as pore size distribution, BET surface area and total pore volume. And the mild shearing force applied in synthesis was the reason causing the special morphology of SM [14], the mild force field slightly affected the hydrolization and condensation of silica source, the formation of primary particles [25–27], but made no difference on the textural properties of final product. After phase separation, however, the secondary arrangement of primary particles was dramatically influenced by the external force field [26,27], and these particles were cross-linked to form net framework finally. In addition, monolithic shape with certain mechanical strength enabled the direct utilization of the composite without further molding process, avoiding the alteration of natural textual properties. Consequently, SM sample exhibited its superiority in adsorption as described below.

3.2. Instantaneous adsorption and catalytic degradation of nitrosamines in laboratory

Table 1 and Fig. 5 describe the gaseous adsorption of NPYR on SBA-15 and its analogues at 453 K, in which the contact time between the volatile nitrosamines and the adsorbent is less than 0.1 s hence this instantaneous adsorption is employed to assess the adsorptive performance of sample [6,28]. For the pure siliceous materials SBA-15 and SM, it is hard to capture NPYR within so short time because they lack powerful adsorptive sites to attract and to hold the nitrosamines. When the amount of NPYR passed through the adsorbent accumulated to 0.8 mmol g^{-1}, SBA-15 and SM trapped 16% and 13%, respectively (Table 1), since their adsorption relayed on surface silanol groups that had a weak interaction with volatile nitrosamines [6]. The 3D net-like morphology did not improve the adsorption capacity of mesoporous silica toward small molecules in gas stream within a very short contact time. In contrary, coating zirconia on porous materials could provide the strong electrostatic affinity toward the N–N=O group of nitrosamines [15], and 5% ZrO_2/SM adsorbed 86% of NPYR under the same conditions (Table 1). Besides, 5% ZrO_2/SM sample exhibited higher activity than SBA-15 and SM throughout whole adsorption procedure (Fig. 5), indicating the important role played by the zirconium

Table 1
Physicochemical properties of mesoporous silica samples.

Samples	a_0 (nm)[a]	S_{BET} ($m^2\,g^{-1}$)[b]	S_{mic} ($m^2\,g^{-1}$)[c]	V_p (mL g^{-1})[d]	V_{mic} (mL g^{-1})[e]	D_p (nm)[f]	Adsorption of NPYR (%)[g]	Liquid adsorption of NNN (%)[h]
SBA-15	10.4	885	157	1.16	0.062	9.1	16.3	86
SM	11.0	832	141	1.10	0.056	9.1	13.9	96
SM-P	11.0	730	117	0.98	0.046	9.0	–	–
5%ZrO_2/SM	10.9	705	149	0.91	0.061	8.9	86.3	93

[a] The lattice parameter calculated from $a_0 = d_{100} \times 2/3^{1/2}$.
[b] BET surface area.
[c] Micropore area.
[d] Total pore volume.
[e] Micropore volume.
[f] BJH mesopore diameter calculated from the adsorption branch.
[g] The accumulated amount of NPYR passed on sample at 453 K was 0.8 mmol g^{-1}.
[h] The concentration of NNN solution was 1.1 mg mL^{-1}.

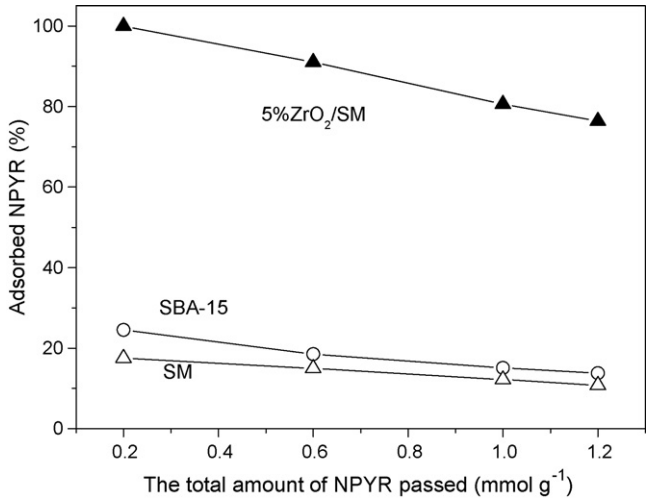

Fig. 5. Adsorption of NPYR by SBA-15 samples at 453 K.

cation in the instantaneous adsorption of volatile nitrosamines. Different situation was observed in the liquid adsorption of NNN at 277 K, in which the adsorbent had enough time to contact with the nitrosamines. The advantage of 3D net-like morphology emerged in the liquid adsorption, and SM sample trapped 10% more NNN than SBA-15 (Table 1). Electrostatic factor also influences liquid adsorption of nitrosamines [29,30], but seems to have minor effect on the mesoporous material with 3D net-like morphology, because SM and 5% ZrO_2/SM samples possessed similar adsorption capability in the solution. This phenomenon is different from that of powder-like mesoporous silica where incorporation of metal oxide considerably enhanced the adsorption [31], implying the morphology effect of materials in the liquid adsorption as discussed later.

Fig. 6A shows the temperature programmed surface reaction (TPSR) results of SBA-15, SM and 5% ZrO_2/SM samples to evaluate their catalytic ability for the degradation of volatile nitrosamines. NPYR consists of 5 membered ring and its degradation starts from the rupture of N–NO bond to release nitric oxygen product [32,33]. TPSR is another routine to assess the adsorptive and catalytic performance of molecular sieves, in which the sample should trap the nitrosamines in gas flow at relative low temperature and then catalyze their degradation at elevated temperature [17], and the detected nitrogen oxides represented the amount of nitrosamines degraded in the thermal process. SBA-15 had weak activity to degrade NPYR, and only 7 $\mu mol\,g^{-1}$ NOx were detected accompanied with the climax of NOx desorption around 493 K. SM sample exhibited the same climax (493 K) in the NOx desorption profile but the amount of NOx detected increased to 12 $\mu mol\,g^{-1}$, 70% more than that of SBA-15, and these NOx products emerged in a wider range of temperature, from 430 K to 650 K. Both SBA-15 and SM were pure siliceous mesoporous silica so this difference should originate from their morphological difference. The special 3D net-linked morphology enabled SM to trap more NPYR in the gas stream at the relatively lower temperature, similar to that observed in liquid adsorption of NNN as mentioned above (Table 1). Coating zirconia on the sample of SM caused a dramatic promotion on its catalytic performance. There were 31.4 $\mu mol\,g^{-1}$ of NOx to be detected on 5% ZrO_2/SM in the range of 430–750 K, with a climax around 532 K. The shifted temperature of climax from 493 K to 523 K reflected the strengthened adsorption of NPYR or NOx on the modified sample, due to the function of zirconia modifier that was the powerful adsorptive and catalytic sites of nitrosamines [15]. Based on these results, it is clear that coating metal ions through dry-impregnation pathway is an efficient way to improve

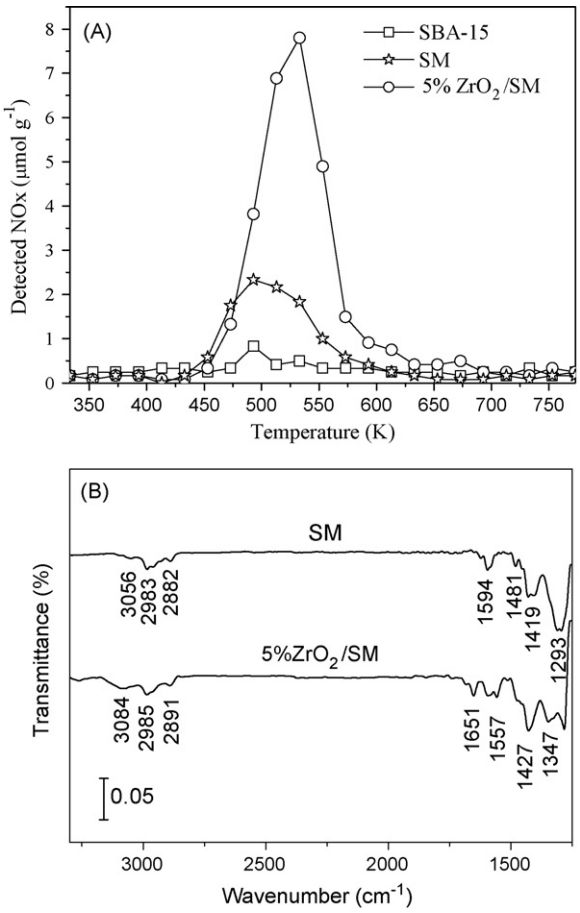

Fig. 6. (A) the profile of NOx detected in the temperature programmed surface reaction (TPSR) of NPYR and (B) in situ FTIR spectra of NNN on SBA-15 mesoporous silica samples.

the adsorptive and catalytic properties of 3D net-linked SBA-15 monolith without damaging its special morphology.

Fig. 6B is the in situ FTIR spectrum of NNN adsorbed on the sample of SM and 5% ZrO_2/SM. No difference was observed between SBA-15 and SM samples in this experiment because the sample discs should be pressed under high pressure, in which 3D net-linked morphology of SM sample was drastically destroyed therefore the test of SBA-15 sample was omitted. Contrarily, the influence of metal ions on the adsorption of nitrosamines was clearly observed. NNN could be adsorbed by SM sample to give the bands at 3056, 2983, 2882, 1594, 1481, 1419 and 1293 cm^{-1}, attributed to the characteristics of NNN molecule [5,28], with some minor shifts owing to host–guest interaction. Three new peaks at 1651, 1557, 1347 cm^{-1} bands of NO_2^- [34] and ν_3 (NO_2) [35] emerged in the spectrum of NNN adsorbed on 5% ZrO_2/SM at 423 K, indicating the decomposition of adsorbed NNN molecules and mirroring the enhanced catalytic activity of the composite. Such improvement had been reported on the zirconia modified zeolites [15], and attributed to the inherent feature of zirconia and the guest–host interaction.

3.3. Actual function of 3D net-linked SBA-15 to capture nitrosamines in complex chemical system

Table 2 lists the reduction of smoke components by SBA-15 with different morphology. As expected, SM was active to lower the tar content of smoke while SBA-15 was inactive. Tar relates to the particles in smoke with the main size of μm [7] that exceeds the pore

Table 2
Reduction of the components in mainstream smoke by SBA-15 with different morphology.

Samples	TPM (mg cig^{-1})[a]	CO (mg cig^{-1})	Water (mg cig^{-1})	Nicotine (mg cig^{-1})	Tar (mg cig^{-1})
Control	17.80	14.4	2.95	1.39	13.51
SBA-15	16.91	14.5	2.98	1.31	12.67
SM	15.83	14.6	3.03	1.21	11.64
SM-P	17.60	14.5	2.88	1.33	13.44
5%ZrO_2/SM	13.93	14.2	2.65	1.05	10.28

[a] Total particular materials in smoke.

size of SBA-15, so that all of zeolites and common mesoporous silica fail to filter these particles [3,14]. Likewise, SM-P lost the ability of trapping particles in smoke, inactive as SBA-15, and failed to reduce both TPM and tar value of smoke (Table 2), which further proven the crucial function of 3D net-linked framework in filtering particles in gas stream. Coating zirconia on SM sample enhanced its ability of reducing tar content (Table 2), hence 10% more of tar along with 11% more of particles (represented by the value of TPM in Table 2) was removed from the smoke. However, 5% ZrO_2/SM also reduced both nicotine and water contents of smoke, different from SMA-15 and SM, which might originate from the changed surface state of the sample caused by zirconia modifier to create the selectivity toward some components in smoke. For this reason, succeeding tests would be focused on SM sample though the zirconia modified analogue was able to reduce nitrosamines content of smoke [14].

Table S1 depicts the influence of SM additive amount on the reducing particles in smoke. The value of TPM and tar in smoke continually declined as the additive amount rose from 5 to 20 mg cig^{-1} while the content of CO, nicotine and water vibrates slightly. When the amount of additive increased to 25 mg cig^{-1}, the tar content of smoke decreased dramatically, accompanied by the obvious decline of nicotine and water contents, because a mass of tar covered the surface of SM to strengthen the trap of nicotine and water. Consequently, the amount of SM additive in succeeding experiments was limited in the range of 5–25 mg cig^{-1}. Table 3 demonstrates the reduction of TSNA level in smoke by using different amount of SM in the filter of cigarette, in comparison with the decrease of total particular materials (TPM) to check the actual performance of this sample in reducing nitrosamines level of smoke. When 5 mg cig^{-1} of SM sample was added into the filter, the TSNA level of smoke declined about 14% meanwhile the TPM value kept unchanged within the experimental error. Among 4 representative TSNA, NNN was reduced 13%, NNK deceased 9%, NAB + NAT declined 61%. As the adding amount of SM increased to 15 mg cig^{-1}, the reduction of TSNA achieved 33% but TPM value was lowered 9%, suggesting the selective removal of TSNA by SM sample. Concerning the components of TSNA, NNN lowered 29%, NNK reduced 34% and NAB + NAT decreased 72%. When 25 mg cig^{-1} of SM sample were used in filter, the TSNA content and TPM value were lowered 48% and 19%, respectively (Table 3). Among components of TSNA, NNN was removed 55%, NNK was eliminated 45% while 11% of NAB + NAT were reduced. No doubt SM sample, the 3D net-linked mesoporous silica trapped more TSNA than TPM in smoke indeed, exhibiting the special selective adsorption toward tobacco specific nitrosamines in smoke, similar to that found on zeolite-like calcosilicate CAS-1 [3].

Table 3
Reduction of TSNA content in the mainstream smoke of Virginia type cigarette by use of 3D net-linked SBA-15 (SM).

Sample	Control	SM		
	0[a]	5[a]	15[a]	25[a]
Pressure drop (mm Hg H_2O)	930	902	1035	1122
TPM (mg cig^{-1})	17.8	18.3	16.2	14.3
CO (mg cig^{-1})	15.1	14.9	15.1	15.3
NNN (ng cig^{-1})	1.58	1.37	1.12	0.71
NNK (ng cig^{-1})	1.21	1.10	0.80	0.66
NAT + NAB (ng cig^{-1})	0.18	0.07	0.05	0.16
Total amount (ng cig^{-1})	2.97	2.54	1.97	1.53
Reduction (%)				
NNN	0	13	29	55
NNK	0	9	34	45
NAT + NAB	0	61	72	11
TSNA (A)	–	14.5	33.7	48.5
TPM (B)		−2.8	9.0	19.7
A − B	–	17.3	24.7	28.8

[a] Added amount (mg cig^{-1}).

4. Discussion

Morphology of molecular sieve materials, either microscopic or macroscopic, is important for their adsorptive and catalytic applications, especially in the environmental adsorption and catalysis in which the trace amount of targets was accompanied with a larger number of other components. The catalyst should capture the targets among the vast compounds through selective adsorption at first, and then catalyze their reactions. However, morphology-control is the inherent drawback of molecular sieves, especially the macroscopic morphology, and most of them, zeolites or mesoporous silica samples are powder-like materials hence they have to be molded with adhesive, not only increasing their costs but also decreasing their performances. Consequently, a lot of effort has been devoted to develop the porous silica materials with mold appearance [36–39], and we also develop the new meso-structured monolith for CO_2 adsorption recently [40]. Nonetheless, the difficulty in removal of carcinogens in environmental tobacco smoke (ETS) requires the special functional materials with 3D net-linked morphology, because the targets are TSNA that adhere on the particles in smoke, and the average diameters of these particles exceed the pore size of zeolite or mesoporous silica therefore these molecular sieves failed to reduce the TSNA level of smoke [3,14], though they could efficiently trap the volatile nitrosamines in smoke that exist in vapor phase instead of particular phase [4]. To overcome this problem, new materials should be prepared and more important, a new concept should be established to realize the selective capture of target, in this paper it is TSNA, in the complex chemical system.

Cellulose acetate and activated carbon are able to trap the particles in smoke, but they cannot selectively adsorb TSNA so that nitrosamine yields appear to follow the trends in particles yields [7]. The reason, as we aforementioned, is that cellulose acetate lacks active site to chemically adsorb TSNA while activated carbon cannot capture TSNA unless it traps the particle on which the TSNA adheres. To perform the selective adsorption of TSNA, the adsorbent should have soft collision with the particle and capture the TSNA from the particle, and then allow the particle to escape (Scheme 1). Clearly the adsorbent ought to have the net-linked morphology together with a suitable flexibility. For this aim we prepared SM sample through adjusting the parameters of synthesis. It is not difficult to get the primary rod-like particles of SBA-15 in synthesis, but is hard to make them run parallel to the long axis end to end;

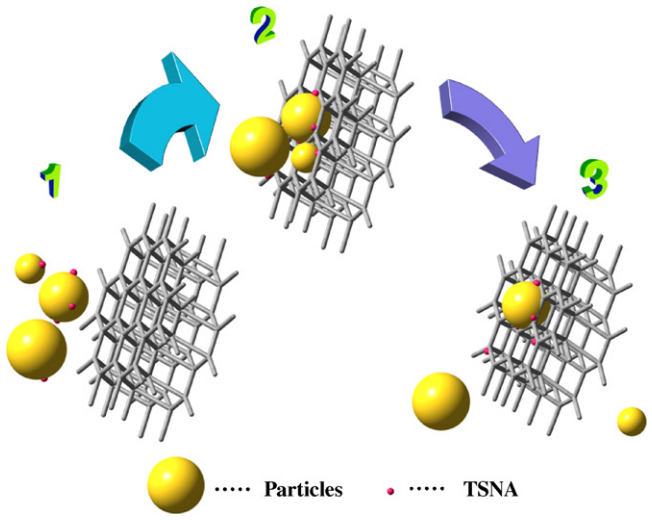

Scheme 1. The possible mechanism of selective capturing TSNA by 3D net-linked framework.

for example, the rods of SBA-15 are rulelessly arranged to form separately and loosely assembled bundles with various length (Fig. 2A and Fig. S2A). We tried to control the hydrolysis rate of siliceous source by using tetramethyl orthosilicate (TMOS) in synthesis [14], and stirred the solution very slowly so that these rod-like particles of SBA-15 could suspend in the solution, parallel-aligned and cross-linked each other, forming the 3D net-linked morphology and finally aggregating the monolith. Thanks to the suitable chemical composition tailoring the hydrolysis of reactant along with the physical factor adjusting the appropriate stirring rate, new environmental adsorbent is developed with the ordered mesopores and 3D net-linked morphology plus the monolith shape (Fig. 1). Ordered mesostructure endows the material the selectivity in adsorption, 3D net-linked morphology enables the material to trap the particles with μm size, and the monolith shape provides the device application to the material since it can be directly sieved to small part for use (in present study it is used as additive in filter) without molding. The latter two new functions of SM sample will expand the potential application of molecular sieves in environment protection and other relative fields, since the application of device is the weak point of molecular sieves for long time.

SM sample has the same chemical composition to SBA-15 so it did not show any advantage in the instantaneous adsorption of NPYR at 453 K (Table 1 and Fig. 5). However, SM became more active in the adsorption at relatively low temperature, for instance in the TPSR process and liquid adsorption. Rather, SM sample realized the selective capture of TSNA in smoke (Table 3), not only confirming the feasibility of our new concept, but also providing more information on the function of morphology in selective adsorption. In general, morphology and surface state of molecular sieve affect the selective reduction of TSNA in smoke. The special net-linked morphology enables the porous material to capture the large particles in smoke, hence zeolites and mesoporous silica materials were inactive but cotton-like CAS-1 was active to filter the particles in smoke [3]. Apart from different morphology, however, CAS-1 owned different cation (Ca^{2+}) from zeolites such as NaA and KA, which made the function of morphology in CAS-1 difficult to be evaluated. Here, SBA-15 and SM have almost same textural property, the same chemical composition but different morphology so it is clear that different performance of two samples in capturing the particles of smoke results from their morphology. This conclusion was also confirmed by SM-P sample that lost the filtering capacity (Table 2) once its 3D net-linked framework was smashed under high pressure (Fig. 2B). Two possible factors may account for the selective adsorption of TSNA by SM sample. Firstly, special 3D net-linked morphology provided the soft-collision between the additive and the particles in smoke, enabling the particles to be hold, even tentatively within a short time, by the adsorbent in which TSNA will enter into the channel and separate from the particles. When the particle escapes from the adsorbent for some reasons, it has been filtered. Secondly, the net-linked morphology of the adsorbent is able to change the orientation of smoke passing through and elongates the contact time between particle and adsorbent [3,14]. During this process, the quantum limitation effect of the mesopore and the surface silanol group will play a key role for the selective adsorption, which differs from the physical filtering in cellulose acetate. The possibility of catalysis was excluded because the filter additive worked in ambient temperature at which the degradation of nitrosamines could not occur according to the results of TPSR (Fig. 6A). Although some nitrosamines could be decomposed at room temperature on acidic zeolites [29], lack of active sites on SM sample obviated this possibility.

At first glance, SM and CAS-1 samples have different morphology, the former is 3D net-linked and the latter is interlaced fiber-like. However, their similar filtering capacity of particular materials in smoke implies the comparability of their morphology. In fact, the 3D net-linked framework of SM is a kind interlaced fiber-like morphology with better regulation, and the interlaced fiber-like morphology of CAS-1 also formats a kind net. It is the special net-like morphology to remedy the inherent drawback of micropores and mesopores that cannot accommodate the particulates with μm size. In addition, cotton-like CAS-1 and monolithic SM sample can be simply broken to small particles, omitting the press-mold process, so that they keep their net-like morphology thanks to their inherent macromorphology. Nonetheless, SM sample has the selective adsorption property different from CAS-1. In the case that additive amount was below 15 mg cig^{-1}, SM emphatically reduced the tar content of smoke (Table S1); whilst CAS-1 trapped tar, water and nicotine in smoke without selectivity [3]. The difference originated from different surface states of two samples. Existence of Ca^{2+} and K^{+} in the structure of CAS-1 [13] yielded its hydrophilicity and strong electrostatic attraction, while the siliceous framework of SM leaded to hydrophobicity. Besides, SM sample needs shorter time and simpler procedure than CAS-1 in synthesis, providing the available candidate for environmental adsorption.

In general, adsorption is the necessary step of heterogeneous catalysis, but catalysis is more important than adsorption for environment protection, because through which the pollutant can be degraded or converted to form less harmful compounds. Clearly the catalytic activity of SM sample is very low because of its pure siliceous composition hence modification is inevitable. Dry impregnation was selected among various modification methods to preserve the special morphology of SM sample, and zirconia was chosen as the guest due to its excellent performance in the modification of zeolites [15]. Nitrosamines are the target in present research, and all of them have a N–NO group with negative charge that is easily attracted by the cation in adsorbent [5,17,28], therefore introducing the cation with high valence such as Al^{3+} or Zr^{4+} on mesoporous silica is efficient to enhance its activity in the adsorption and catalytic degradation of nitrosamines. As expected, 5% ZrO_2/SM showed a much higher adsorptive capacity of NPYR in the instantaneous adsorption (Fig. 5), along with the catalytic activity several times higher than SM in TPSR test (Fig. 6A). Moreover, it could degrade NNN even in the FTIR measurement (Fig. 6B). However, 5% ZrO_2/SM did not adsorb more NNN in solution (Table 1) due to two reasons. The first, Zr is mainly homogeneously distributed throughout the sample from the X-ray mapping (the top images of Fig. S3); moreover, when elemental mapping of single rod that recorded in the magnification of 22,000 illustrates that the

Zr distribution is not accord with Si and O distribution (the bottom images of Fig. S3), indicating that many zirconia modifiers were coated on the external surface of rod-like particles that linked each other; otherwise, the Zr distribution should be the same as that of Si and O. These external modifiers had minor influence to promote the adsorption of nitrosamines inside the channel of sample. The second, liquid adsorption of NNN provided a long enough time for adsorbent to contact with nitrosamines and achieve adsorption equilibrium, in which the silanol group of mesoporous silica could play the role of adsorptive site [6,29]; therefore the promotion of zirconia modifier on the adsorption capacity of SM sample was unconscious.

Apart from the promotion on the instantaneous adsorption of volatile nitrosamines such as NPYR, coating zirconia on SM sample also varied the surface property of the adsorbent to improve the capture of tar and nicotine in smoke. However, the adsorption of water in smoke was not enhanced (Table 2), which was different from microporous materials such as zeolite and activated carbon. This phenomenon implies that mesoporous silica materials may be the more suitable candidate than microporous materials for the selective adsorption in complex system such as environment tobacco smoke (ETS), due to their inherent tunable structure and facility of modification. In fact, this zirconia modified sample also exerted the function to eliminate volatile nitrosamines in smoke, which is another challenge for mesoporous materials in environment protection, and the reduction reached 38% [14]. Nonetheless, this composite ought to be used as catalyst at elevated temperature, instead of as adsorbent at ambient temperature, so that it had not been tested as the filter additive and would be applied in some environmental catalysis procedures in future.

5. Conclusion

It is feasible to control the morphology of mesoporous silica through tuning the synthetic conditions, influencing the hydrolization and condensation of silica source, the formation and the secondary arrangement of primary particles, finally forming the monolith with 3D net-linked morphology. It is also possible to introduce zirconia guest on the monolith through dry-impregnation method, without damage of 3D net-linked morphology.

Owning to the special 3D net-linked micromorphology and monolithic macroscopic shape, the sample SM can efficiently intercept the particles of smoke though these particles possess the μm size exceeding the pore diameter of molecular sieves. Moreover, SM sample can selective capture the TSNA adhered on these particles in smoke, capturing more TSNA species than the particles.

3D net-linked framework improved the performance of mesoporous silica in liquid adsorption of nitrosamines. Surface modification of SM sample with zirconia strengthens the electrostatic affinity toward nitrosamines, increasing the capability in adsorption of NPYR and elevating the catalytic activity in degradation of NPYR and NNN.

The above studies illustrate the influence of morphology and surface states on the elimination of carcinogenic compounds by molecular sieves in complex environment, giving the suggestion for preparing novel environmental adsorbent and catalyst through morphology controlling.

Acknowledgements

Financial support from 863 Program of the MST of China (2008AA06Z327), NSF of China (20773601, 20873059 and 20871067), Jiangsu Provincial Natural Science Foundation Industrial Supporting Program (BE2008126), Jiangsu Province Environmental Protection Bureau Scientific Research Program (2008005), the Scientific Research Foundation of Graduate School, Grant CX08B_009 from Jiangsu Province Innovation for PhD candidate and Analysis Center of Nanjing University is gratefully acknowledged. The authors are grateful to Technology Centers of Shandong Tobacco Group and Jiangsu Tobacco Group for their technical assistances.

Appendix A. Supplementary data

Supplementary data associated with this article can be found, in the online version, at. doi:10.1016/j.cattod.2010.04.052.

References

[1] P.D. Terry, T.E. Rohan, Cancer Epidemiol. Biomarkers Prev. 11 (2002) 953.
[2] H. Vainio, E. Weiderpass, P. Kleihues, Toxicology 166 (2001) 47.
[3] L. Gao, Y. Cao, S.L. Zhou, T.T. Zhuang, Y. Wang, J.H. Zhu, J. Hazard. Mater. 169 (2009) 1034.
[4] L. Gao, Y. Wang, Y. Xu, S.L. Zhou, T.T. Zhuang, Z.Y. Wu, J.H. Zhu, Clean: Soil Air Water 36 (2008) 270.
[5] Y. Cao, Z.Y. Yun, J. Yang, X. Dong, C.F. Zhou, T.T. Zhuang, Q. Yu, H.D. Liu, J.H. Zhu, Micropor. Mesopor. Mater. 103 (2007) 352.
[6] C.F. Zhou, Y.M. Wang, Y. Cao, T.T. Zhuang, W. Huang, Y. Chun, J.H. Zhu, J. Mater. Chem. 16 (2006) 1520.
[7] R.R. Baker, in: D.L. Davis, M.T. Nielsen (Eds.), Tobacco Production, Chemistry and Technology, Blackwell Science, London, 1999, pp. 419–428.
[8] D.W. Eaker, Rec. Adv. Tob. Sci. 16 (1990) 103.
[9] K. Nakajima, M. Okamura, J.N. Kondo, K. Domen, T. Tatsumi, S. Hayashi, M. Hara, Chem. Mater. 21 (2009) 186.
[10] P. Ratnasamy, D. Srinivas, Catal. Today 141 (2009) 3.
[11] A. Bordoloi, S. Sahoo, F. Lefebvre, S.B. Halligudi, J. Catal. 259 (2008) 232.
[12] C.F. Xue, G.H. Liu, J.P. Li, J.X. Dong, in: S.H. Feng, J.S. Chen (Eds.), Frontiers of Solid State Chemistry, World Scientific, Singapore, 2002, pp. 233–240.
[13] J.L. Jorda, S. Prokic, L.B. McCusker, C. Baerlocher, C.F. Xue, J. Dong, C. R. Chim. 8 (2005) 331.
[14] Y. Zhou, L. Gao, F.N. Gu, J.Y. Yang, J. Yang, F. Wei, Y. Wang, J.H. Zhu, Chem. Eur. J. 15 (2009) 6748.
[15] T.T. Zhuang, J.H. Xu, J.R. Xia, Y. Cao, S.L. Zhou, Y. Wang, H.D. Liu, Y. Chun, J.H. Zhu, J. Nanomater. 2006 (2006), doi:10.1155/JNM/2006/54909 (Article ID 54909, 9 pages).
[16] D.Y. Zhao, Q.S. Huo, J.L. Feng, B.F. Chmelka, G.D. Stucky, J. Am. Chem. Soc. 120 (1998) 6024.
[17] Y. Xu, J.H. Zhu, L.L. Ma, A. Ji, Y.L. Wei, X.Y. Shang, Micropor. Mesopor. Mater. 60 (2003) 125.
[18] Z.Y. Wu, H.J. Wang, T.T. Zhuang, L.B. Sun, Y.M. Wang, J.H. Zhu, Adv. Funct. Mater. 18 (2008) 82.
[19] International Organisation for Standardisation (1991). ISO 3308: Routine analytical cigarette-smoking machine: Definition and standard condition.
[20] K. Kosuge, T. Sato, N.I. Kikukawa, M. Takemori, Chem. Mater. 16 (2004) 899.
[21] D.Y. Zhao, J.Y. Sun, Q.Z. Li, G.D. Stucky, Chem. Mater. 12 (2000) 275.
[22] A. Katiyar, S. Yadav, P.G. Smirniotis, N.G. Pinto, J. Chromatogr. A 1122 (2006) 13.
[23] P.S. Winkel, P.D. Yang, D.I. Margolese, B.F. Chmelka, G.D. Stucky, Adv. Mater. 11 (1999) 303.
[24] M. Kruk, M.J.H. Ko, R. Ryoo, Chem. Mater. 12 (2000) 1961.
[25] P. Linton, V. Alfredsson, Chem. Mater. 20 (2008) 2878.
[26] F. Kleitz, F. Marlow, G.D. Stucky, F. Schüth, Chem. Mater. 13 (2001) 3587.
[27] C.Z. Yu, J. Fan, B.Z. Tian, D.Y. Zhao, Chem. Mater. 16 (2004) 889.
[28] J. Yang, Y. Zhou, H.J. Wang, T.T. Zhuang, Y. Cao, Z.Y. Yun, Q. Yu, J.H. Zhu, J. Phys. Chem. C 112 (2008) 6740.
[29] C.F. Zhou, Z.Y. Yun, Y. Xu, Y.M. Wang, J. Chen, J.H. Zhu, New J. Chem. 28 (2004) 807.
[30] J. Yang, X. Dong, Y. Zhou, M.B. Yue, C.F. Zhou, F. Wei, J.H. Zhu, C. Liu, Micropor. Mesopor. Mater. 120 (2009) 381.
[31] F.N. Gu, Y. Zhou, F. Wei, Y. Wang, J.H. Zhu, Micropor. Mesopor. Mater. 126 (2009) 143.
[32] J.-P. Cheng, M. Xian, K. Wang, X. Zhu, Y. Zheng, P.G. Wang, J. Am. Chem. Soc. 120 (1998) 10266.
[33] K. Hiramoto, Y. Ryuno, K. Kikugawa, Mutat. Res. 520 (2002) 103.
[34] M. Sirilumpen, R.T. Yang, N. Tharapiwattenanon, J. Mol. Catal. A: Chem. 137 (1999) 273.
[35] J. Szanyi, M.T. Paffett, J. Catal. 164 (1995) 232.
[36] J. Babin, J. Iapichella, B. Lefevre, C. Biolley, J.P. Bellat, F. Fajulaa, A. Galarneau, New J. Chem. 31 (2007) 1907.
[37] Q.S. Huo, J.L. Feng, F. Schuth, G.D. Stucky, Chem. Mater. 9 (1997) 14.
[38] H.P. Lin, C.Y. Mou, Acc. Chem. Res. 35 (2002) 927.
[39] C. Chen, S.T. Yang, W.S. Ahn, R. Ryoo, Chem. Commun. (2009) 3627.
[40] J.J. Wen, F.N. Gu, F. Wei, Y. Zhou, W.G. Lin, J. Yang, J.Y. Yang, Y. Wang, Z.G. Zou, J.H. Zhu, J. Mater. Chem. 20 (2010) 2040.